UNIVERSITI MALAYSIA PERLIS
International Journal of Nanoelectronics and Materials
IJNeaM
ISSN 1985-5761 | E-ISSN 2232-1535

Novel composite corn starch-graphene oxide-based polymer electrolyte with the addition of cerium nitrate to improve its ionic conductivity

Nur Laila Hamidah [a] *, Nabilah Idriana Permata Putri [a], Fernando Wijaya [a], Sylvia Ayu Pradanawati [b], and Lukman Noerochim [c]

[a]Engineering Physics, Institut Teknologi Sepuluh Nopember, Surabaya 60111, Indonesia
[b]Mechanical Engineering, Universitas Pertamina, Jakarta 12220, Indonesia
[c]Materials and Metallurgical Engineering, Institut Teknologi Sepuluh Nopember, Surabaya 60111, Indonesia
∗ Corresponding author. Tel.: +62 881-9889-016; e-mail: nurlaila@its.ac.id

Received 17 December 2024, Revised 19 March 2025, Accepted 09 April 2025

ABSTRACT

Solid polymer electrolytes (SPE) offer a safer alternative to liquid electrolytes in electrochemical applications, driving interest in enhancing their ionic conductivity. This study examined the impact of adding cerium nitrate ($Ce(NO_3)_3$) to a composite SPE to boost conductivity. SPEs were synthesized from corn starch, $Ce(NO_3)_3$ salt, and graphene oxide (GO) via solution casting, using $Ce(NO_3)_3$ variations of 0%, 2.5%, 5%, 7%, and 9%. X-ray diffraction (XRD) analysis indicated a structural shift toward amorphousness with increasing salt, which enhances ionic mobility. Fourier transform infrared (FTIR) analysis revealed narrowing of the O-H peak with starch and GO, implying hydrogen bonding that promotes an amorphous phase. At the CH_2OH peak, salt addition suggested interaction with starch. Scanning electron microscopy (SEM) showed a porous composite morphology conducive to ion movement. Thermogravimetric analysis (TGA) confirmed good thermal stability. Electrochemical impedance spectrometry (EIS) results showed an increase in ionic conductivity in SPE due to the addition of $Ce(NO_3)_3$ with the highest conductivity value observed at the 9% variation, reaching 39 times higher than those without $Ce(NO_3)_3$. This study highlights significant improvements in ionic conductivity by incorporating $Ce(NO_3)_3$ into SPE, enhancing the energy storage system's performance. The research offers valuable insights into developing advanced SPE materials with superior electrochemical properties for further exploration and innovation in the field of electrochemical devices.

Keywords: *Cerium, Graphene oxide, Ionic conductivity, Solid polymer electrolyte*

1. INTRODUCTION

An Energy Storage System (ESS) is a system that can convert electrical energy into another form of energy, which may then be stored in a storage medium and converted back into electricity as needed. When the demand for electrical energy is low, the ESS stores it and releases it when the demand rises [1]. Batteries are a regularly used technology in ESS. There are different sorts of batteries, with lithium-ion batteries being one of the most extensively utilized nowadays. This technology works by moving Li-ions from the cathode to the anode during the charging process and from the anode to the cathode during the discharging process [2]. Batteries generally use liquid electrolytes, but liquid electrolytes have the disadvantage of having a higher leakage rate compared to solid electrolytes. To solve this issue, Solid Polymer Electrolytes (SPE) have been developed as solid electrolytes because they offer advantages such as flexibility, no leakage, and easy processing [3]. However, at room temperature, SPEs have low ionic conductivity and low lithium-ion migration [3]. Despite this, SPE have good plasticity and flexibility, allowing them to be molded as needed [3]. There are various types of SPE materials that can be used, but polyethylene oxide (PEO) and polyvinylpyrrolidone (PVP) are the most widely used materials because they have higher electrochemical stability than other polymer electrolytes [4]. However, PEO has the disadvantage of low conductivity at room temperatures [4]. PVP has excellent electrical properties, but it has the limitations of poor film-forming ability [5]. Various types of starch are used to develop SPE. Starch contains two polysaccharides: amylose and amylopectin. Amylose is a sparsely branched carbohydrate, whereas amylopectin is a highly branched polymer with a high molecular weight, contributing to its crystallinity [6]. Common natural sources of starch are cassava, potatoes, and corn. Each type of starch has different amylose content: cassava (18—20% amylose), potatoes (17—21% amylose), and corn (22—30% amylose) [6]. Among the types of starch developed, corn starch has the lowest degree of crystallinity, which can influence the high conductivity of the film [7]. Corn starch is a semi-crystalline polymer composed of linear amylose and branched amylopectin linked by glycosidic bonds. Its structure has made it the focus of many studies aiming to develop stable, high-ionic-conductivity polymer electrolytes as alternatives to conventional types [7]. However, most natural polymers have very low film conductivity, so to enhance conductivity, many researchers have conducted studies to improve it, such as adding salts to the polymer electrolytes or incorporating ionic liquids into the polymer electrolytes [3]. The addition of salt makes the SPE more amorphous, facilitating the segmental motion of ions, thus increasing the ionic conductivity of the SPE [3]. Several studies have discussed the effect of salt on the ionic conductivity of SPE. Research has been conducted by adding $NaClO_4$ salt [4] and cerium-based solid electrolyte salt, which can reduce grain boundary resistance, thereby increasing ionic conductivity significantly [8]. Another method being developed to increase the conductivity of SPE is the addition of Graphene Oxide (GO). GO is a two-dimensional material consisting of oxygen-functionalized carbon atoms covalently bonded. GO has a high conductivity level due to its rich oxygen functional groups [9]. Typically, GO's structural model shows that the edges of its sheets are primarily composed of ionizable carboxylic acid groups and are hydrophilic, making GO interact easily with other compounds [9]. According to research, cerium salt modification of GO can significantly enhance conductivity because cerium salt ions slow down the desorption of oxygen functional groups and maintain the interlayer spacing at higher temperatures [10]. The interaction between cerium salt and GO can change from C-O-C to C-O-H [10]. Thus, this work investigates the effect of incorporating cerium salt into corn starch-GO-based SPE composites on enhancing their conductivity.

2. METHODS

To achieve the objectives of this study, several steps must be carried out, including the synthesis and characterization of SPE. The first step is synthesizing GO and the SPE, followed by the second step, which involves characterizing the synthesized SPE. This characterization includes X-ray diffraction (XRD), Fourier transform infrared spectroscopy (FTIR), scanning electron microscopy (SEM), thermogravimetric analysis (TGA), and electrochemical impedance spectroscopy (EIS).

2.1. GO Synthesis Process

GOs were synthesized using Tour Method with modification [10]. 3 g of expanded graphite (Ito Graphite Co., Ltd., Japan with a median diameter of 5-50 μm) and 18 g of $KMnO_4$ were mixed in a solution of 360 mL H_2SO_4 and H_3PO_4 with volume ratio 9:1. After that the mixture was stirred at 50°C for 12 hours. The mixture was cooled to 25°C and then 6 mL of H_2O_2 was added to the mixture. The mixture was centrifuged to obtain solid products, which were then washed with HCl and distilled water. The solid products were subsequently dispersed in distilled water and ultrasonicated for 5 h to produce GO through exfoliation, then centrifuged at 10000 rpm for 10 minutes to collect GO nanosheets and redispersed in distilled water for further use.

2.2. Solid Polymer Electrolyte (SPE) Synthesis Process

SPE was fabricated using the solution casting method. Five variations were prepared: corn starch 2 grams with 25 ml distilled water, with cerium salt ($Ce(NO_3)_3$ MERCK, German crystalline powder with solubility of 1754 g/L) from variations of 0%, 2.5%, 5%, 7%, and 9%, and with GO at 0.5 wt.%. The maximum amount of $Ce(NO_3)_3$ concentration that can be completely dissolved in the SPE solution is 9%. The amount of $Ce(NO_3)_3$ in wt.% can be calculated using Equation (1):

$$\text{wt\%} = \frac{x}{x+y} 100 \qquad (1)$$

where x is the weight of the salt (g), y is the weight of the polymer, and the weight percentage is the difference in salt percentage as a dopant.

The fabrication process of SPE was carried out by sonicating GO with 25 ml distilled water until dissolved. Various amounts of $Ce(NO_3)_3$ at 0%, 2.5%, 5%, 7%, and 9% were sequentially added to the sonicated GO solution until dissolved, using a magnetic stirrer. Glycerol was then added, followed by the addition of 2 grams of corn starch, which was stirred again. After complete dissolution, the solution was stirred using a magnetic stirrer and hot plate within a water bath at a temperature of 80°C to 90°C until homogeneous. The mixture was then cooled until no bubbles were present, poured into a petri dish, and dried in an oven at 50°C until the SPE film formed. The fabrication process of Solid Polymer Electrolyte (SPE) can be seen in Figure 1.

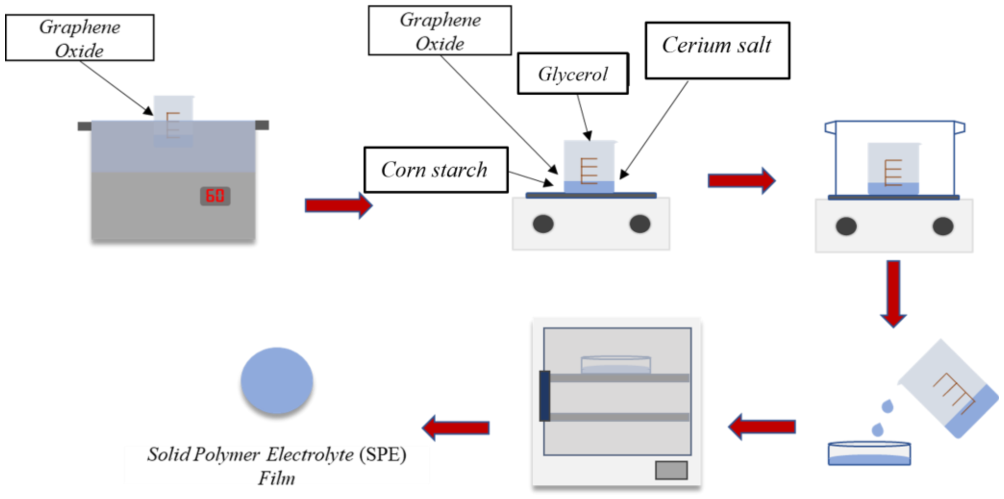

Figure 1. Fabrication process of SPE

2.3. Material Characterization

The produced SPE film was tested using XRD, FTIR, SEM, TGA, and EIS. XRD analysis was conducted using a Pan Analytical XRD E'xpert PRO with CuKα wavelengths of 1.54056 Å and Ni filters was operated at 40 kV and 100 mA to determine the crystallinity of the SPE film. Measurements were taken in the 2θ range of 5—80°, with a scanning speed of 0.5°C/min and 0.05°/step at room temperature. FTIR analysis using the Thermo Scientific Nicolet iS10 type was used to discover ionic or functional group interactions between corn starch-GO and $Ce(NO_3)_3$ salt in the SPE. SEM characterization with the FEI Inspect S50 model was used to examine the surface morphology of the SPE film. TGA using Mettler Toledo with a scan rate of 10°C, temperature range 25—600°C was used to determine the thermal stability of SPE.

2.4. Electrochemical Characterization

EIS using Corrtest type CS Series Electrochemical Workstation to perform AC impedance spectroscopy with a frequency range from 1 MHz – 1 Hz and a signal of 10 mV. EIS was utilized for electrochemical characterization aimed at analyzing the ion conductivity of the SPE film. The conductivity of the SPE film was determined using Equation (2):

$$\sigma = \frac{l}{R_b A} \qquad (2)$$

where σ represents conductivity (S/cm), l is the sample thickness, A is the surface area of the film, and R_b is the bulk resistance (Ω).

3. RESULTS AND DISCUSSION

Synthesis of SPE using corn starch as the polymer, 0.5% GO as the filler, and $Ce(NO_3)_3$ salt with variations of Ce at 0%, 2.5%, 5%, 7%, and 9%. Figure 2 shows the synthesis results of SPE with variations of Ce at 0%, 2.5%, 5%, 7%, and 9%.

Figure 3 shows the XRD test results with variations of $Ce(NO_3)_3$ salt at 0%, 2.5%, 5%, 7%, and 9%. The results indicate that there are 4 peaks of corn starch, which appear at angles of approximately 15.25°, 17.09°, 18.10°, and 23.02°. These corn starch peaks are of type A and then change to type B after adding glycerol. The corn starch peaks before adding glycerol have a double peak at angles 17.09° and 18.10°, and after adding glycerol, they exhibit the characteristics of type B starch peaks at an angle of 19°.

Plasticizing starch with glycerol leads to the destructuring of its crystalline regions, causing the type A peak characteristics to disappear in the diffraction pattern when glycerol is added [11]. The difference between type A and B starch relates to the number of water molecules that stabilize the helices [12]. Type A structure is monoclinic with four water molecules per unit cell, while type B structure can accommodate more water molecules per unit cell [12]. The GO compound has a peak at an angle of 10.6° [13], and in the XRD results, no GO peak is observed with the addition of 0.5% GO for samples with 0%, 2.5%, and 9% Ce, indicating that the GO has mixed perfectly [13]. $Ce(NO_3)_3$ has peaks at angles of 22°, 31.4°, and 77.7°. The starch peaks after adding glycerol and GO have peaks at angles of 17°, 19°, and 21°.

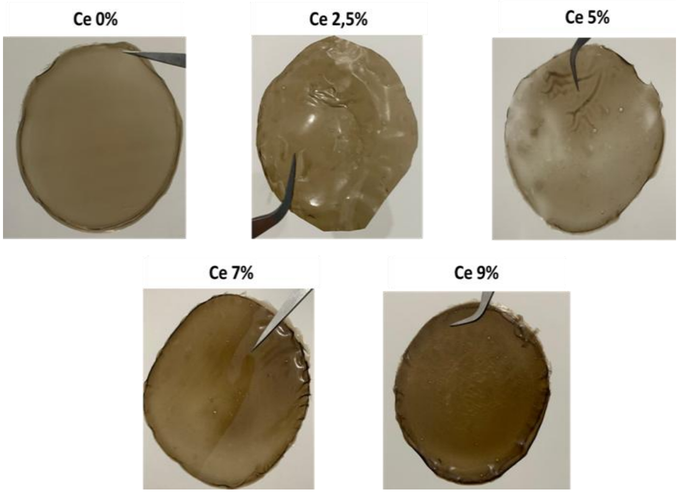

Figure 2. Synthesis results of SPE with variations of Ce at 0%, 2.5%, 5%, 7%, and 9%

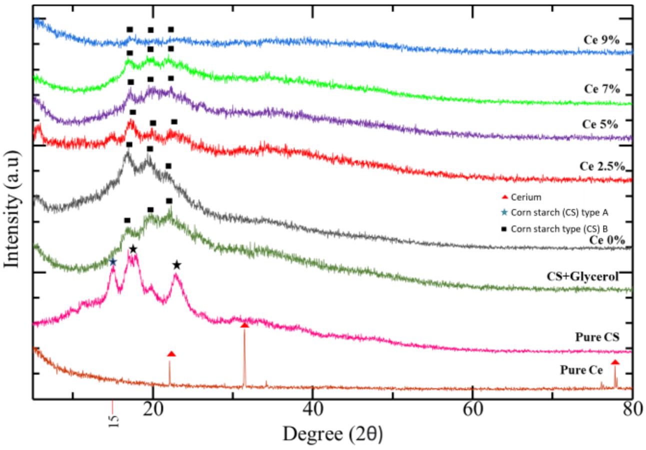

Figure 3. XRD test results with variations of $Ce(NO_3)_3$ salt at 0%, 2.5%, 5%, 7%, and 9%

The addition of $Ce(NO_3)_3$ salt in the XRD graph shows a decreasing intensity, indicating that the higher the salt concentration, the more amorphous the sample becomes. Amorphousness occurs due to the interaction between the polymer chains and the salt, which will be observed in FTIR [14]. This is seen in the starch peak with the addition of 2.5% $Ce(NO_3)_3$ experiencing a decrease in intensity. Then, with the addition of 9% $Ce(NO_3)_3$ salt, the intensity of the starch peak decreases when compared to Ce 2.5%, Ce 5%, and Ce 7%.

Thus, it is found that among all SPE films, Ce 9% is more amorphous. The amorphous phase in polymer electrolytes is critical as it helps increase the ionic conductivity of the electrolyte, where the amorphous phase has greater ionic diffusion, resulting in better conductivity [15]. Therefore, samples with a more amorphous phase are expected to produce high conductivity values. This can be attributed to the rapid segmental movements of the polymeric backbone in the amorphous area, which enhance the mobility of charge carriers and facilitate ionic conductivity [16].

The results from FTIR analysis are used to identify ionic interactions in functional groups by detecting the formation or breaking of functional group bonds. Figure 4(a) shows the FTIR characterization graph of the SPE film in the range of 4000-400 cm^{-1}. The identification results of functional groups in the SPE film can be seen in Table 1. At 3290 cm^{-1} to 3304 cm^{-1}, O-H stretching bonds are observed, then at 1077, 1149, and 997 cm^{-1}, there is the combination of C-O, C-C, and asymmetric stretching of the glycosidic bridge [17]. At 1650 cm^{-1}, bending vibration of the OH group occurs [18]. The characteristic peak of corn starch at 1374 cm^{-1} shows a decrease in intensity with the addition of salt in the SPE film [19].

Figure 4(b) shows the enlarged FTIR characterization graph in the range of 1500-1200 cm^{-1}. The bonds at the peak of 1300 to 1500 cm^{-1} are C-H and C-H$_2$ deformations [13]. Around 1327, there is an increase in peak intensity due to the addition of Ce(NO$_3$)$_3$. Around 1327, there is an increase in peak intensity due to the addition of Ce(NO$_3$)$_3$. It is possible that starch reacts with Ce^{3+} at the OH in CH$_2$OH. This interaction can occur because Ce^{3+}, which is a Lewis acid, can accept electron donors from the Lewis base OH, forming a bond [20]. In Figure 4(a) at the wavelength of 3290 cm^{-1}, the O-H peak results from overlapping vibrations between the O-H stretching groups in amylose within starch molecules and GO [21]. At 1020 cm^{-1} indicates C-O-H deformation [22].

In corn starch with the addition of GO, the hydroxyl peak of corn starch at 3304 cm^{-1} shifts to 3290 cm^{-1} with a decrease in peak intensity. The broad peak at 3290 cm^{-1} is associated with the O-H peak, resulting from overlapping vibrations between the O-H stretching groups in amylose within starch molecules and GO.

A decrease in intensity at 1200-800 cm^{-1} is observed for starch mixtures, indicating the cleavage of amylose glycosidic bonds. Changes in FTIR peaks due to hydrogen bonding effects on vibration elements indicate interactions between corn starch material and GO [23]. Consequently, at 1650 and 3290 cm^{-1}, the peaks become narrower when starch with glycerol is added with GO, indicating hydrogen bonding, which can lead to an amorphous phase in the SPE film. The proposed mechanism scheme between corn starch, GO, and Ce(NO$_3$)$_3$ is shown in Figure 5.

SEM characterization was conducted to determine the morphology of the SPE film. The results from SEM characterization at 1000x magnification are shown in Figure 6. The Ce 0% sample has a smooth surface and appears to have no voids or cracks. White spots visible on the SPE sample indicate that there is starch in the sample that is not yet perfectly homogeneous [24]. The addition of Ce(NO$_3$)$_3$ salt shows that the surface of the SPE composite becomes rougher and more porous, as shown in Figure 6. The addition of pores will allow ions to easily pass through the membrane, potentially leading to increased conductivity [7].

Table 1. Functional groups in the SPE film

Wavenumber (cm^{-1})	Functional Groups
3304 – 3290	O-H stretching
2927	C-H stretching bands
1650	OH groups stretching and bending
1416	CH deformation in CH$_2$-OH
1327	CH$_2$ deformation in CH$_2$-OH
1149	Stretching vibration C-O in C-O-H
1077	Stretching vibration C-O in C-O-H
1020	C-O-H deformation
997	C-O stretching in C-O-C groups

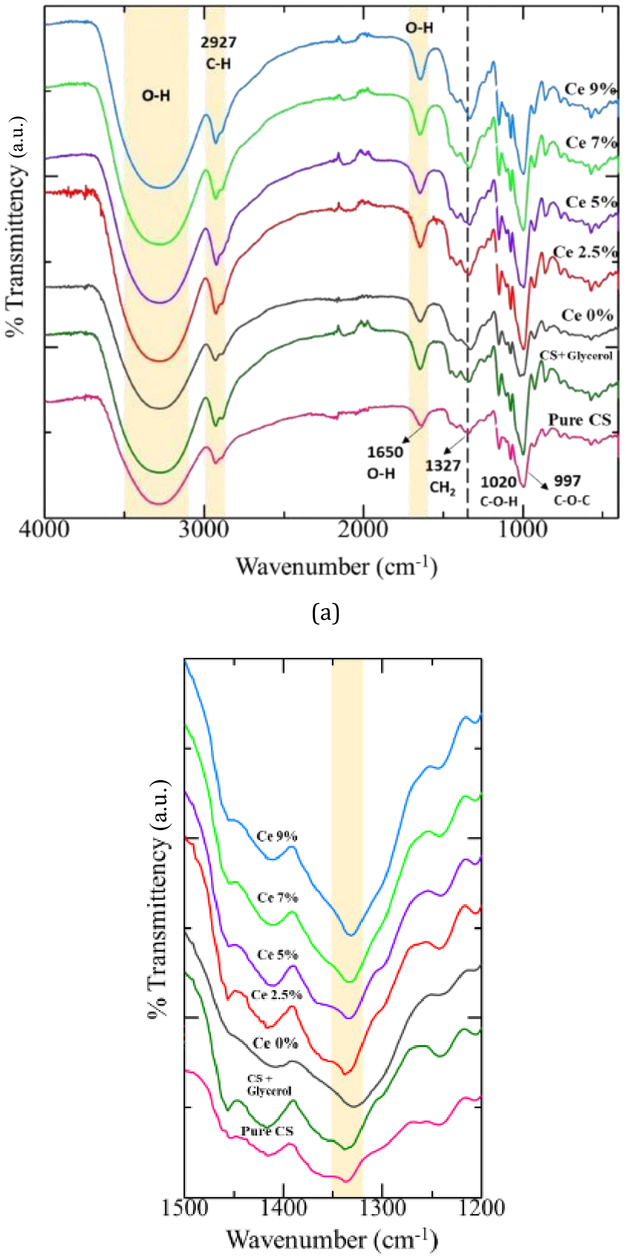

(a)

(b)

Figure 4. FTIR result for (a) 4000-400 cm^{-1} and (b) 1500-1200 cm^{-1}

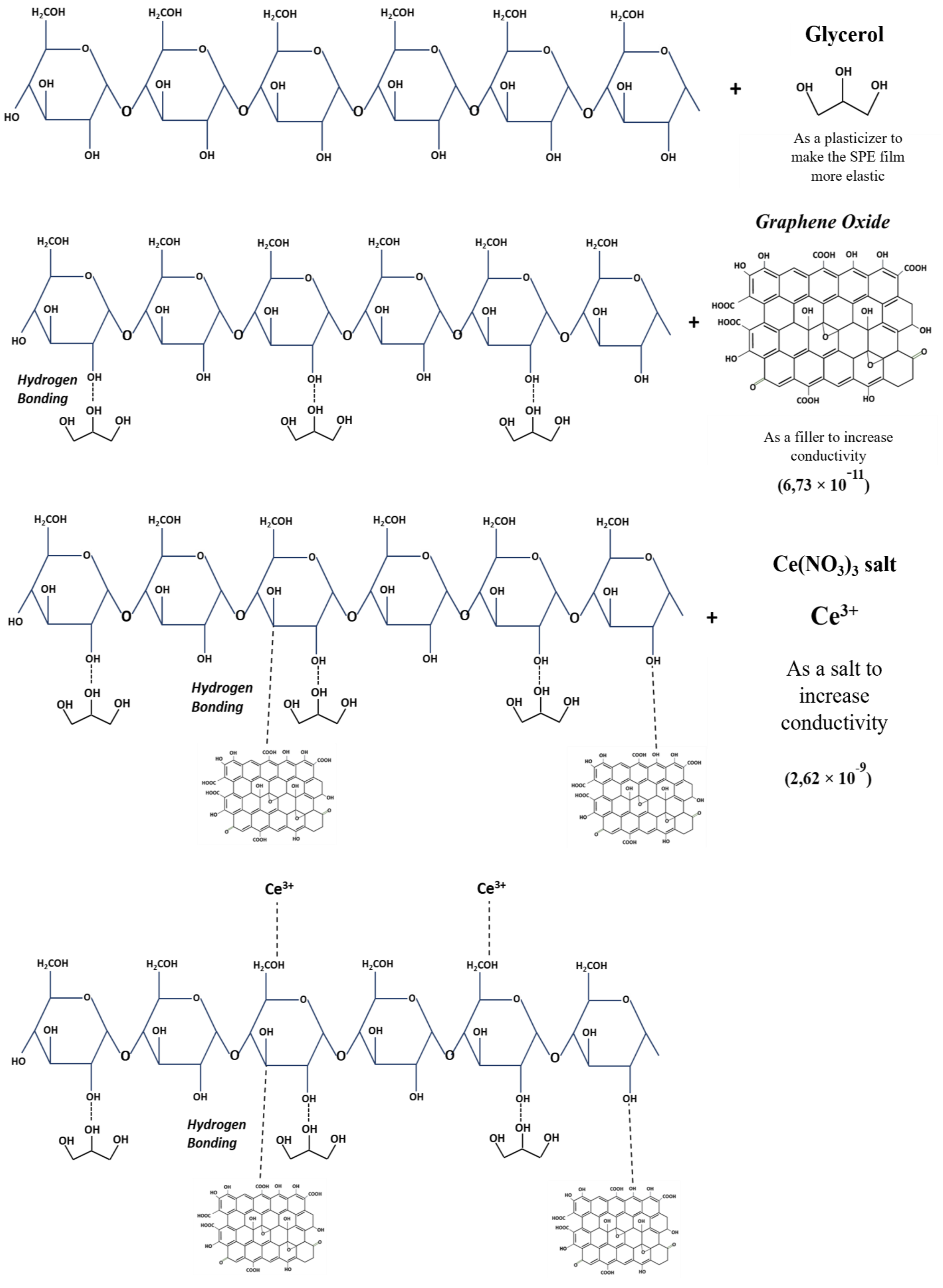

As a plasticizer to make the SPE film more elastic

As a filler to increase conductivity

($6{,}73 \times 10^{-11}$)

As a salt to increase conductivity

($2{,}62 \times 10^{-9}$)

Figure 5. Proposed mechanism scheme between corn starch, GO, and Ce(NO$_3$)$_3$ [20]

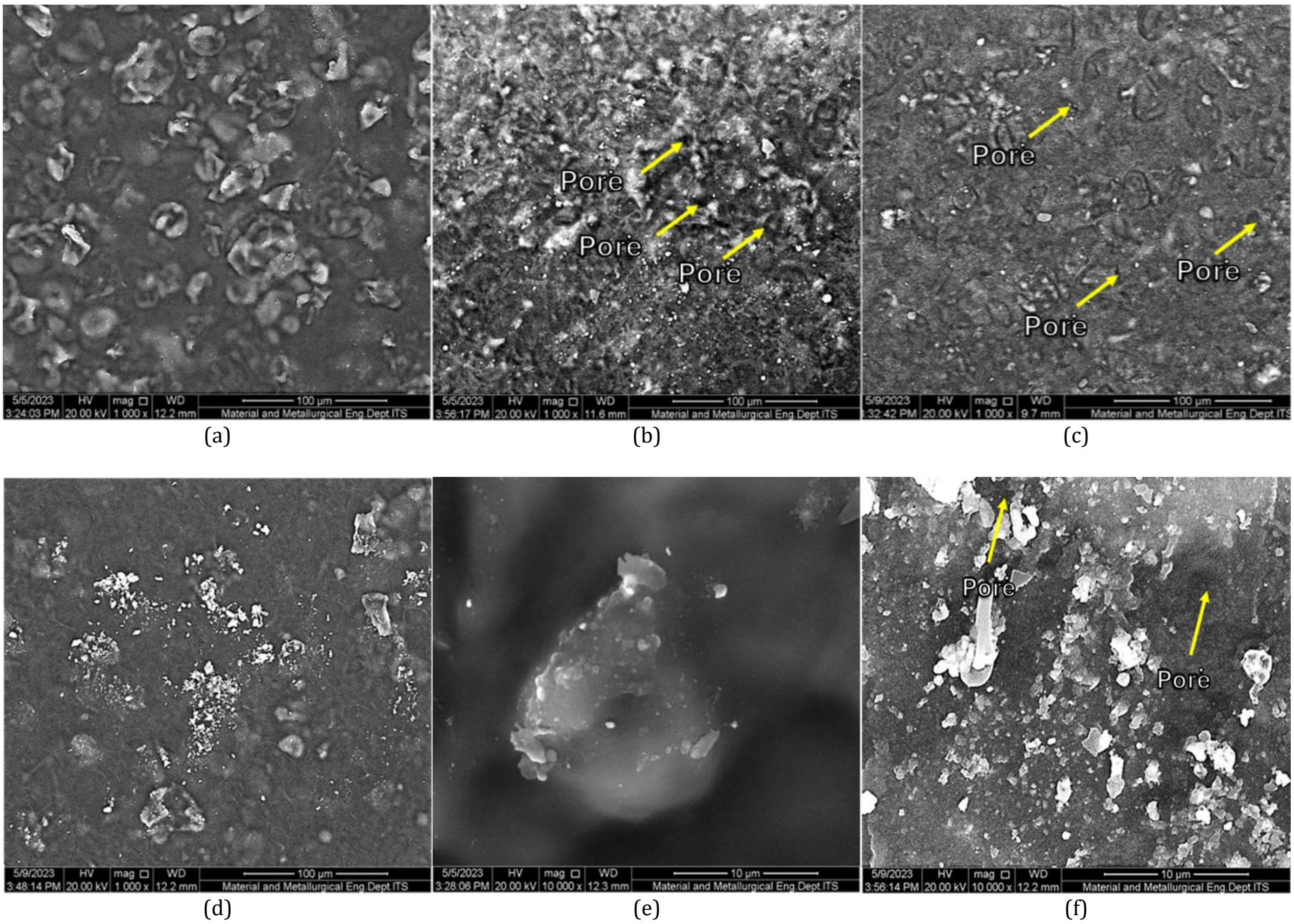

(a) (b) (c)

(d) (e) (f)

Figure 6. SEM results of SPE films at 1000x magnification for (a) Ce 0%, (b) Ce 2.5%, (c) Ce 5%, (d) Ce 9%, and at 10,000x magnification for (e) Ce 0% and (f) Ce 9%

Figures 6(e) and (f) show the SEM results at 10,000x magnification for the Ce 0% and Ce 9% samples, respectively, with Figure 6(f) highlighting the porosity caused by the addition of $Ce(NO_3)_3$.

TGA characterization was conducted to determine whether the addition of $Ce(NO_3)_3$ could result in changes in thermal decomposition behavior. Figure 7(a) shows the TGA characterization graph of the SPE film with variations of

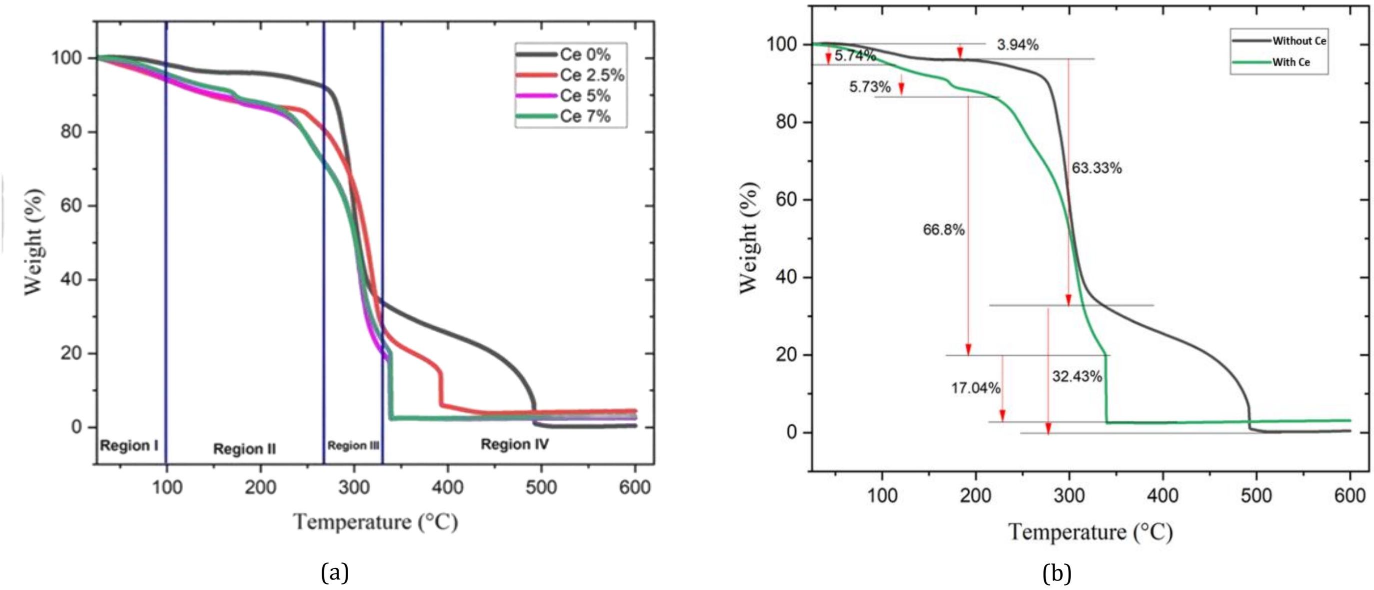

(a) (b)

Figure 7. (a) TGA results and (b) TGA mass loss

Ce 0%, Ce 2.5%, 5%, and Ce 7%, and Figure 7(b) shows the mass reduction values for the Ce 0% and Ce 7% samples.

Region I represents the first decomposition occurring before 100°C due to water loss. The mass reduction in the Ce 0% sample was 3.94%, while in the Ce 7% sample, it was 7.85%. The higher the salt content, the more water is lost compared to samples with lower salt concentrations. This occurs due to the hydrophilic properties of the salt [25]. In Region II, the Ce 7% sample experienced a mass reduction of 5.73%. Region II represents the mass reduction related to the salt-starch bond in the temperature range of 100—180°C [25]. In Region III, the Ce 0% sample experienced a mass reduction of 63.33%, and the mass reduction in the Ce 7% sample was 66.8%. Region III is related to starch degradation [26]. In Region IV, the Ce 0% sample had a residue mass of 32.43%, and the Ce 7% sample had a residue mass of 17.04%.

Table 2 shows the decomposition temperatures of the SPE film with variations of Ce 0%, Ce 2.5%, 5%, and Ce 7%. The decreasing decomposition temperatures with increasing $Ce(NO_3)_3$ indicate that the more crystalline a polymer is, the more energy is required to break the bonds in the polymer [19].

Figure 8(a) displays the results of an EIS test to measure the ionic conductivity of SPE. It was discovered that increasing the amount of $Ce(NO_3)_3$ salt caused a narrower semicircle in the Nyquist plot, indicating increased ionic conductivity in the SPE film.

Ionic conductivity is calculated using bulk resistance, which is obtained from the EIS test results in the form of a Nyquist plot. Figure 8(b) illustrates how an analogous circuit is used to fit the Nyquist plot and calculate the bulk resistance. Ionic conductivity is determined by overall ionic mobility and the amount of charge carriers.

Using Equation (2) to calculate ionic conductivity, the results indicate that ionic conductivity increases with salt content, with Ce 9% exhibiting the highest conductivity at 2.62×10^{-9} S/cm compared to variations of Ce 0%, Ce 2.5%, Ce 5%, and Ce 7%. Figure 9 shows the graph of increasing ionic conductivity in the SPE film with variations of Ce 0%, Ce 2.5%, Ce 5%, Ce 7%, and Ce 9%. The increase in ionic conductivity with the increase in the amount of $Ce(NO_3)_3$ is due to the amorphous phase, as the amorphous phase has higher ionic diffusion, resulting in better conductivity [15].

Table 2. The decomposition temperature of the SPE film

Sample	Initial decomposition temperature (°C)	Final decomposition temperature (°C)
Ce 0.0%	273	492.0
Ce 2.5%	246	393.0
Ce 5.0%	180	339.8
Ce 7.0%	172	339.6

Higher ionic conductivity makes it easier for ions to travel between polymer chains. In electrochemical systems like batteries and supercapacitors, higher ionic conductivity facilitates quicker ion movement, which accelerates the charging and discharging process [27]. Furthermore, increased conductivity leads to longer cycle stability and a reduced internal resistance [28].

Ionic mobility is shown in Figure 10, which is a scheme of ion movement with segmental motion on polymer chain bonds. The decrease in crystallinity in the polymer

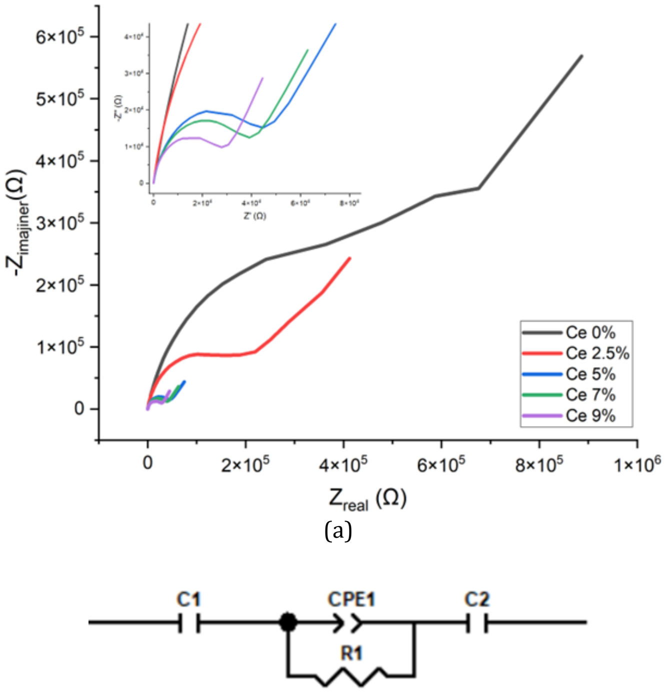

(a)

(b)

Figure 8. (a) Nyquist plot graph of SPE sample and (b) equivalent circuit

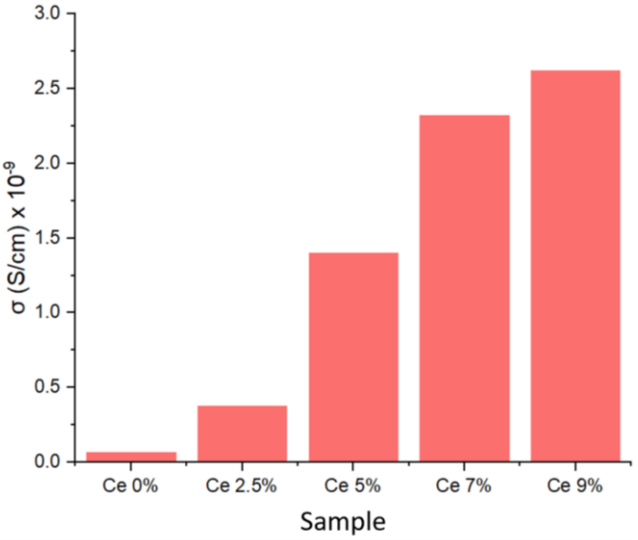

Figure 9. Trend of conductivity increase in SPE

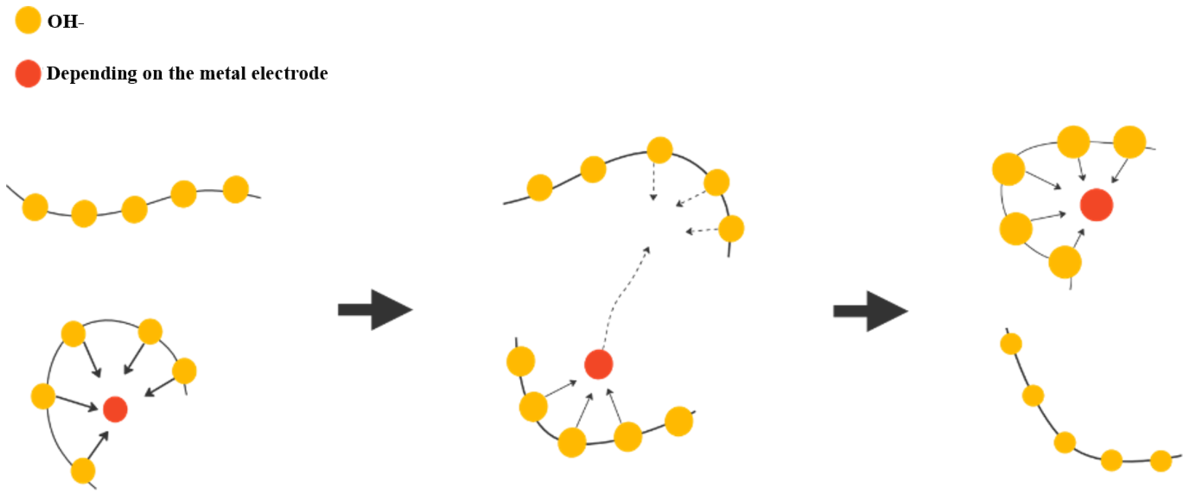

Figure 10. Scheme of ion movement with segmental motion on polymer chain bonds

increases segmental motion because the crystalline regions of the polymer have an orderly and dense structure, restricting polymer chain movement. The more amorphous the polymer, the easier it is for the polymer chains to move, leading to increased segmental motion. Easier polymer chain movement can increase ionic conductivity, as moving polymer chains create spaces that can be filled by ions and coordinated with -OH groups. These ions continue to move, filling the spaces created by the polymer chains during the ion transfer process [29].

4. CONCLUSION

The addition of $Ce(NO_3)_3$ salt to SPE using corn starch and GO causes the SPE film to become more amorphous, as shown by the XRD data. Based on the FTIR results, the starch is going to get more amorphous because of the interaction between $Ce(NO_3)_3$ and the starch's OH groups, as well as hydrogen bonding between GO and starch. Furthermore, SEM characterization data suggest that the addition of $Ce(NO_3)_3$ salt increases the porosity of the SPE film surface. TGA characterization shows that the decomposition temperature decreases as the amount of $Ce(NO_3)_3$ increases, implying that the more crystalline a polymer, the more energy is required to break the polymer's bonds. According to the characterization results, adding $Ce(NO_3)_3$ makes the starch more amorphous, thus enhancing its conductivity.

The addition of $Ce(NO_3)_3$ salt to SPE with corn starch and GO influences the rise in ionic conductivity value. The SPE film with 9% Ce variation has an ionic conductivity of 2.62×10^{-9} S/cm. The rise in ionic conductivity with an increase in the amount of $Ce(NO_3)_3$ is due to the amorphous phase, which has greater ionic diffusion, resulting in higher conductivity.

ACKNOWLEDGMENTS

This work was supported by the Institut Teknologi Sepuluh Nopember under project scheme of the Publication Writing and IPR Incentive Program (PPHKI).

REFERENCES

[1] C. K. Das, O. Bass, G. Kothapalli, T. S. Mahmoud, and D. Habibi, "Overview of energy storage systems in distribution networks: Placement, sizing, operation, and power quality," *Renewable and Sustainable Energy Reviews*, vol. 91, pp. 1205–1230, Aug. 2018, doi: 10.1016/j.rser.2018.03.068.

[2] D. Deng, "Li-ion batteries: basics, progress, and challenges," *Energy Science & Engineering*, vol. 3, no. 5, pp. 385–418, Sep. 2015, doi: 10.1002/ese3.95.

[3] M. S. M. Misenan and T. Eren, "Solid Polymer Electrolyte: A Review," in *International Eurasian Conference on Biotechnology and Biochemistry (BioTechBioChem 2020)*, 2020, pp. 254–260.

[4] Y. L. Ni'mah, M.-Y. Cheng, J. H. Cheng, J. Rick, and B.-J. Hwang, "Solid-state polymer nanocomposite electrolyte of TiO_2/PEO/$NaClO_4$ for sodium ion batteries," *Journal of Power Sources*, vol. 278, pp. 375–381, Mar. 2015, doi: 10.1016/j.jpowsour.2014.11.047.

[5] S. A, S. R. Manohara, and L. Gerward, "Influence of polyvinylpyrrolidone on optical, electrical, and dielectric properties of poly(2-ethyl-2-oxazoline)-polyvinylpyrrolidone blends," *Journal of Molecular Liquids*, vol. 247, pp. 328–336, Dec. 2017, doi: 10.1016/j.molliq.2017.09.086.

[6] D. Seung, "Amylose in starch: towards an understanding of biosynthesis, structure and function," *New Phytologist*, vol. 228, no. 5, pp. 1490–1504, Dec. 2020, doi: 10.1111/nph.16858.

[7] F. F. Awang, M. F. Hassan, and K. H. Kamarudin, "Corn starch doped with sodium iodate as solid polymer electrolytes for energy storage applications," *Acta Polytechnica*, vol. 61, no. 4, pp. 497–503, Aug. 2021, doi: 10.14311/AP.2021.61.0497.

[8] N. Jaiswal, K. Tanwar, R. Suman, D. Kumar, S. Upadhyay, and O. Parkash, "A brief review on ceria based solid electrolytes for solid oxide fuel cells," *Journal of Alloys and Compounds*, vol. 781, pp. 984–1005, Apr. 2019, doi: 10.1016/j.jallcom.2018.12.015.

[9] A. M. Dimiev and S. Eigler, Eds., *Graphene Oxide:*

Fundamentals and Applications. Wiley, 2016. doi: 10.1002/9781119069447.

[10] N. L. Hamidah *et al.*, “Graphene Oxide Membranes with Cerium-Enhanced Proton Conductivity for Water Vapor Electrolysis,” *ACS Applied Nano Materials*, vol. 3, no. 5, pp. 4292–4304, May 2020, doi: 10.1021/acsanm.0c00439.

[11] M. Paluch, J. Ostrowska, P. Tyński, W. Sadurski, and M. Konkol, “Structural and Thermal Properties of Starch Plasticized with Glycerol/Urea Mixture,” *Journal of Polymers and the Environment*, vol. 30, no. 2, pp. 728–740, Feb. 2022, doi: 10.1007/s10924-021-02235-x.

[12] S. Pérez, P. M. Baldwin, and D. J. Gallant, “Structural Features of Starch Granules I,” in *Starch*, Elsevier, 2009, pp. 149–192. doi: 10.1016/B978-0-12-746275-2.00005-7.

[13] A. A. Azli, N. S. A. Manan, and M. F. Z. Kadir, “The development of Li^+ conducting polymer electrolyte based on potato starch/graphene oxide blend,” *Ionics*, vol. 23, no. 2, pp. 411–425, Feb. 2017, doi: 10.1007/s11581-016-1874-z.

[14] F. N. Jumaah, N. N. Mobarak, A. Ahmad, M. A. Ghani, and M. Y. A. Rahman, “Derivative of iota-carrageenan as solid polymer electrolyte,” *Ionics*, vol. 21, no. 5, pp. 1311–1320, May 2015, doi: 10.1007/s11581-014-1306-x.

[15] M. F. Norjeli, N. Tamchek, Z. Osman, I. S. Mohd Noor, M. Z. Kufian, and M. I. B. M. Ghazali, “Additive Manufacturing Polyurethane Acrylate via Stereolithography for 3D Structure Polymer Electrolyte Application,” *Gels*, vol. 8, no. 9, p. 589, Sep. 2022, doi: 10.3390/gels8090589.

[16] N. H. A. Rosli, C. H. Chan, R. H. Y. Subban, and T. Winie, “Studies on the Structural and Electrical Properties of Hexanoyl Chitosan/Polystyrene-based Polymer Electrolytes,” *Physics Procedia*, vol. 25, pp. 215–220, 2012, doi: 10.1016/j.phpro.2012.03.074.

[17] H. Ismail and N. F. Zaaba, “The mechanical properties, water resistance and degradation behaviour of silica-filled sago starch/PVA plastic films,” *Journal of Elastomers & Plastics*, vol. 46, no. 1, pp. 96–109, Feb. 2014, doi: 10.1177/0095244312462163.

[18] R. Li, C. Liu, and J. Ma, “Studies on the properties of graphene oxide-reinforced starch biocomposites,” *Carbohydrate Polymers*, vol. 84, no. 1, pp. 631–637, Feb. 2011, doi: 10.1016/j.carbpol.2010.12.041.

[19] K. H. Teoh, C.-S. Lim, and S. Ramesh, “Lithium ion conduction in corn starch based solid polymer electrolytes,” *Measurement*, vol. 48, pp. 87–95, Feb. 2014, doi: 10.1016/j.measurement.2013.10.040.

[20] R. Vallesi, “Study of the Lewis acid catalyzed Povarov reaction for the synthesis of polycylic tetrahydroquinoline derivatives,” 2017. [Online]. Available: https://api.semanticscholar.org/CorpusID:233179238

[21] I. Capron, P. Robert, P. Colonna, M. Brogly, and V. Planchot, “Starch in rubbery and glassy states by FTIR spectroscopy,” *Carbohydrate Polymers*, vol. 68, no. 2, pp. 249–259, Mar. 2007, doi: 10.1016/j.carbpol.2006.12.015.

[22] M. F. Ab Rahman, S. R. Yahya, and A. R. Azura, “The Effect of Alkali Treated Native Sago Starch Concentration on Mechanical Properties of Natural Rubber Latex Composite Films,” *Journal of Physics: Conference Series*, vol. 1082, p. 012011, Aug. 2018, doi: 10.1088/1742-6596/1082/1/012011.

[23] E. A. Azimi *et al.*, “Strength Development and Elemental Distribution of Dolomite/Fly Ash Geopolymer Composite under Elevated Temperature,” *Materials*, vol. 13, no. 4, p. 1015, Feb. 2020, doi: 10.3390/ma13041015.

[24] Syaubari, Abubakar, T. M. Asnawi, M. Zaki, M. Khadafi, and I. Harmanita, “Synthesis and characterization of biodegradable plastic from watermelon rind starch and chitosan by using glycerol as plasticizer,” *Materials Today: Proceedings*, vol. 63, pp. S501–S506, 2022, doi: 10.1016/j.matpr.2022.04.535.

[25] A. Pawlicka, A. C. Sabadini, E. Raphael, and D. C. Dragunski, “Ionic Conductivity Thermogravimetry Measurements of Starch-Based Polymeric Electrolytes,” *Molecular Crystals and Liquid Crystals*, vol. 485, no. 1, pp. 804–816, Apr. 2008, doi: 10.1080/15421400801918138.

[26] D. Schlemmer, R. S. Angélica, and M. J. A. Sales, “Morphological and thermomechanical characterization of thermoplastic starch/ montmorillonite nanocomposites,” *Composite Structures*, vol. 92, no. 9, pp. 2066–2070, Aug. 2010, doi: 10.1016/j.compstruct.2009.10.034.

[27] L.-L. Lu *et al.*, “Extremely fast-charging lithium ion battery enabled by dual-gradient structure design,” *Science Advances*, vol. 8, no. 17, Apr. 2022, doi: 10.1126/sciadv.abm6624.

[28] E. Lizundia, C. M. Costa, R. Alves, and S. Lanceros-Méndez, “Cellulose and its derivatives for lithium ion battery separators: A review on the processing methods and properties,” *Carbohydrate Polymer Technologies and Applications*, vol. 1, p. 100001, Dec. 2020, doi: 10.1016/j.carpta.2020.100001.

[29] P. Nayak, Y. N. Sudhakar, S. De, Ismayil, and S. K. Shetty, “Optimization of Chitosan: Methylcellulose polyblend to obtain highly amorphous polymer matrix useful for ion transportation,” *Indian Journal of Physics*, vol. 97, no. 12, pp. 3483–3493, Oct. 2023, doi: 10.1007/s12648-023-02684-1.